Fusion Science and Technology

ISSN: 1536-1055 (Print) 1943-7641 (Online) Journal homepage: http://www.tandfonline.com/loi/ufst20

Self-Radiolysis of Tritiated Water: Experimental Study and Simulation

Sylver Heinze, Thibaut Stolz, Didier Ducret & Jean-Claude Colson

To cite this article: Sylver Heinze, Thibaut Stolz, Didier Ducret & Jean-Claude Colson (2005) Self-Radiolysis of Tritiated Water: Experimental Study and Simulation, Fusion Science and Technology, 48:1, 673-679, DOI: 10.13182/FST05-A1014

To link to this article: http://dx.doi.org/10.13182/FST05-A1014

SELF-RADIOLYSIS OF TRITIATED WATER: EXPERIMENTAL STUDY AND SIMULATION

Sylver Heinze[1], Thibaut Stolz[1], Didier Ducret[1], Jean-Claude Colson[2]

[1] *Commissariat à l'Energie Atomique, CEA Valduc, 21120 IS-SUR-TILLE, France. E-mail: sylver.heinze@cea.fr*
[2] *Laboratoire de Recherches sur la Réactivité des Solides, Université de Bourgogne, 21048 DIJON Cedex, France*

Radioactive decay of tritium contained in tritiated water leads to the production of gaseous helium and, through self-radiolysis, to the formation of molecular hydrogen and oxygen. For safety management of tritiated water storage, it is essential to be able to predict pressure increase resulting from this phenomenon. The present study aims to identify the mechanisms that take place in self-radiolysis of chemically pure liquid tritiated water. The evolution of the concentration of hydrogen and oxygen in the gas phase of closed vessels containing tritiated water has been followed experimentally. Simulation of pure water radiolysis has been carried out using data from the literature. In order to fit experimental results, simulation should take into account gas phase recombination reaction between hydrogen and oxygen. A simplified system has been extracted from the complete chemical system used to simulate radiolysis. This system allows identifying the basic mechanisms that are responsible for tritiated water self-radiolysis.

I. INTRODUCTION

In tritium plants, glove-boxes atmosphere is commonly cleaned using catalytic oxidation of tritium in water that is usually trapped onto molecular sieve. Tritiated water could then be stored under various forms: liquid in polyethylene or stainless steel vessels, ice, adsorbed on zeolite. Whatever the storage form, tritium radioactive decay is responsible for both helium production and for radiolysis that lead to molecular hydrogen and oxygen formation. As tritiated water storage vessels are generally tightly closed to avoid tritium scattering in the atmosphere, their inner pressure continuously increases due to the previously described phenomena. Thus, safety management of tritiated water storage requires an extensive knowledge of radiolysis in order to be able to predict the temporal evolution of pressure.

If the production of helium is easily calculable, the mechanisms of tritiated water self-radiolysis are dependent on many parameters: volumic activity, chemical form, dissolved impurities, etc. Moreover, radiolysis of water has been widely investigated in the case of external irradiation by γ rays or α particles[1-3] but only few works have been carried out in the case of self-radiolysis of tritiated water[4].

The purpose of the present study is to identify the mechanisms that are predominant in self-radiolysis of liquid tritiated water in order to be able to establish a predictive model that could be used to improve the safety of storage[5].

The approach of this study, dedicated to chemically pure tritiated water with a volumic activity below 74 $TBq \cdot L^{-1}$ (2,000 $Ci \cdot L^{-1}$), is twofold, combining experiments and simulation. The experiments consist in following the evolution with time of some macroscopic effects of self-radiolysis: concentration of molecular hydrogen and oxygen in the gas phase of a closed system containing liquid tritiated water. On the other hand, simulation takes into account production of reactive species due to radiolysis and chemical reactions that produce molecular products, hydrogen, oxygen and hydrogen peroxide. Confrontation between simulation and experimental data allows the validation of the data used for simulation.

II. TRITIATED WATER, TRITIUM RADIOACTIVE DECAY AND RADIOLYSIS

II.A. Tritiated water

Tritiated water contains three isotopic molecules, H_2O, HTO and T_2O. The proportion of each of these species is determined by equilibrium (1):

$$H_2O + T_2O \rightleftharpoons 2HTO \qquad (1)$$

$K = 3.42$ at 298 K[6].

Moreover, we should notice that "HTO" is also usually used to represent tritiated water, which is the mixture of these three molecules.

In the case of low volumic activity tritiated water, concentration of T_2O is negligible and the proportion of

HTO is very low (e.g. 0.12 % for water at 74 $TBq \cdot L^{-1}$). Tritiated water could then be described as a diluted solution of HTO in light water.

II.B. Tritium radioactive decay in water

Radioactive decay of tritium is described by equation (2):

$$T \rightarrow {}^3He + \beta^- + \bar{\nu} \qquad (2)$$

In the case of tritium atoms contained in tritiated water, radioactive decay is represented by reactions (3) and (4):

$$HTO \rightarrow {}^3He^+ + \beta^- + \bar{\nu} + OH^\bullet \qquad (3)$$

$$T_2O \rightarrow {}^3He^+ + \beta^- + \bar{\nu} + OT^\bullet \qquad (4)$$

In a closed system, helium atoms formed according to these mechanisms cause a pressure increase that could be easily calculated for a given duration from the initial amount of tritium and from the volume of the gas phase.

Furthermore, the energy of β particles formed through tritium radioactive decay (E_{max} = 18.6 keV, $E_{average}$ = 5.7 keV) is enough to break hydrogen – oxygen bonds in water molecules (E_{bond} = 5.2 eV) or to ionise water (E_{ion} = 12.6 eV). The interaction between β particles and water molecules initiates water decomposition through the phenomenon called self-radiolysis.

II.C. Radiolysis of water

Radiolysis of water is a complex phenomenon that has been the object of many studies and reviews[1-3]. The purpose of this paragraph is not to describe mechanisms of water radiolysis in details but to present some fundamental notions.

In radiochemical processes, active species are not produced homogeneously in space but only along the tracks of the incident particles. In the case of β radiation produced by tritium decay, water – particle interaction results in "short tracks" that are finite cylindrical regions. The energy transferred to water molecules causes both ionisation (5) and excitation (6):

$$H_2O \xrightarrow{\beta^-} H_2O^+ + e^- \qquad (5)$$

$$H_2O \xrightarrow{\beta^-} H_2O^* \qquad (6)$$

Electrons released by ionisation become thermalised and hydrated. They are then called aqueous electrons, e^-_{aq} (7):

$$e^- \rightarrow e^-_{th} \rightarrow e^-_{aq} \qquad (7)$$

The H_2O^+ ions react with water molecules according to reaction (8):

$$H_2O^+ + H_2O \rightarrow H_3O^+ + OH^\bullet \qquad (8)$$

Excited water molecules can relax through homolytic dissociation, producing hydrogen and hydroxide radicals (9):

$$H_2O^* \rightarrow H^\bullet + OH^\bullet \qquad (9)$$

Hydrogen and hydroxide radicals can react with other species present in the track forming, among other species, molecular hydrogen and hydrogen peroxide.

The chemical composition of each track changes independently of the other. Radicals and molecular species then diffuse in the solution from the initial track. 10^{-6} s after the energy deposit, it is assumed that the different species are homogeneously distributed in the solution. Their production is quantified using the primary radiolytic yield, G_i, that is defined, for a given product "i", as the number of radicals or molecules formed for 100 eV absorbed.

Primary molecular products of radiolysis are hydrogen and hydrogen peroxide. Further decomposition of hydrogen peroxide leads to oxygen formation. From a macroscopic point of view, considering that the total amount of reactive species is negligible compared to the quantity of molecular products, mass balance of radiolysis could be expressed as:

$$n_{H_2} = 2n_{O_2} + n_{H_2O_2} \qquad (10)$$

where n_X represents the total amount of the "X" molecule.

III. EXPERIMENTS

III.A. Experimental device

Chemically pure tritiated water used in the experiments has been synthesised by isotopic exchange between pure liquid water (resistivy 18.2 MΩ·cm) and gaseous molecular tritium, T_2. Volumic activity of water

was 68 TBq·L^{-1} (1850 Ci·L^{-1}). The pH of water was 6.0 ± 0.5.

The experimental device consists in 450 mL passivated stainless steel vessels filled with 125, 250 or 300 mL of tritiated water. Each vessel is equipped with a Druck 100W-1045 pressure transducer. Temperature in the glove-box is measured using a Pt100 sensor. Temperature, that is not controlled, is 291 ± 3 K.

After water introduction, vessels are tightly closed and partially evacuated up to 50 mbar. Evolution of inner pressure and temperature is then recorded. Samples of the gaseous phase are periodically taken during the experiments and analysed by mass spectrometry to determine the nature and the proportion of the different species. Total pressure, temperature and composition are used to calculate the concentration of each constituent.

III.B. Experimental results

III.B.1. Gas phase composition

As an example of gas phase composition, table I presents the amount of each constituent in this phase (except water vapour that is trapped before mass spectrometry analysis) after 56 days of radiolysis in the case of a vessel containing 300 mL of water. This analysis indicates that this phase is composed of helium 3, produced by tritium decay, nitrogen and argon, coming from the air remaining in the vessels after partial evacuation, hydrogen and oxygen produced by radiolysis. Although water contains tritium, tritiated hydrogen, HT, and molecular tritium, T_2, cannot be detected. In addition, contrary to hydrogen that is only produced by radiolysis, some oxygen is originally present in the vessel. On the other hand, the experimental amount of ^{3}He is coherent with the theoretical value (0.163 mmol).

Table I. Amount of different species in the gas phase after 56 days. 300 mL of water.

Species	Amount (mmol)	Species	Amount (mmol)
T_2	$< 4 \cdot 10^{-4}$	HD	$< 4 \cdot 10^{-4}$
D_2	$< 4 \cdot 10^{-4}$	^{3}He	0.131 ± 0.001
H_2	2.54 ± 0.01	N_2 + CO	$(565 \pm 4) \cdot 10^{-4}$
HT	$< 4 \cdot 10^{-4}$	O_2	1.33 ± 0.01
DT	$< 4 \cdot 10^{-4}$	Ar	$(12 \pm 2) \cdot 10^{-4}$

III.B.2. Evolution of hydrogen and oxygen composition

Figure 1 displays the experimental evolution of concentration of hydrogen and oxygen in the gas phase in the case of vessels containing respectively 300, 250 and 125 mL of tritiated water.

Whatever the volume of water in the vessel, the evolution of the concentration of hydrogen and oxygen presents the same shape. Initially, the production of both species is almost linear and then their rate of production decreases with time.

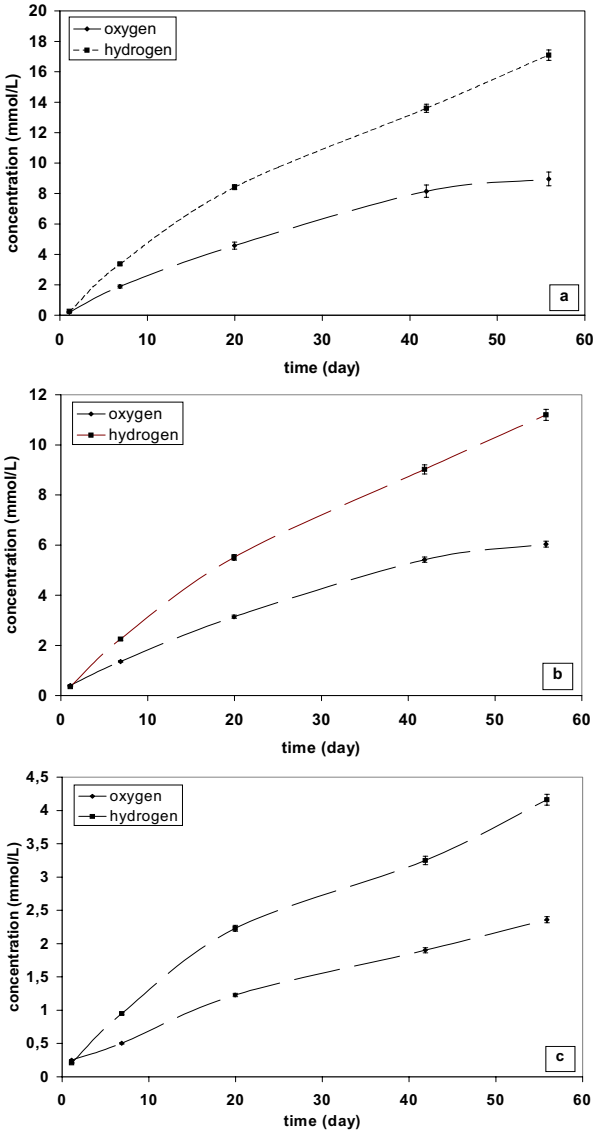

Fig. 1. Experimental evolution of the concentration of hydrogen and oxygen in the gas phase with different volume of water. (a) 300 mL. (b) 250 mL. (c) 125 mL.

At the end of the experiments, the ratio hydrogen/oxygen is respectively 1.95 ± 0.05, 1.92 ± 0.03 and 1.91 ± 0.05 for 300, 250 and 125 mL of water. These values indicate that oxygen is in excess compared to hydrogen. This could be explained by the initial presence of oxygen in the gas phase due to uncompleted evacuation of the vessel. As mentioned above, oxygen is a secondary

product of radiolysis coming from the decomposition of hydrogen peroxide. The concentration of H_2O_2 has been determined experimentally by spectrophotometry. With 300 and 250 mL of water, the concentrations of hydrogen peroxide are respectively $1.3 \cdot 10^{-4}$ and $0.8 \cdot 10^{-4}$ mol·L^{-1}. For the experiment with 125 mL of water, the final concentration of H_2O_2 is below the detection limit of the spectrophotometer, which is $0.6 \cdot 10^{-4}$ mol·L^{-1}. These results indicate that almost all the hydrogen peroxide produced by radiolysis is further decomposed to form molecular oxygen.

IV. SIMULATION

IV.A. Simulation procedure

Simulation of radiolysis is realised thank to the Chemsimul code developed for numerical simulation of the evolution of complex chemical systems under irradiation[7]. This code, conceived for single-phase systems, only considers 0, 1st or 2nd order kinetics. Chemical reactions are treated as differential equations that are numerically resolved. Input data are chemical reactions (radical + radical, radical + molecular species) and their kinetic constants for the considered temperature, acido-basic equilibrium, expressed as two opposite reactions (the ratio of their kinetic constants being equal to the equilibrium constant) and primary radiolytic yields for β rays of tritium. These data are displayed in tables II and III[8-9].

Moreover, as the simulated chemical system is diphasic, we should take into account mass transfer of molecular hydrogen and oxygen between dissolved form and gas phase form. This phenomenon is described by Henry's law. In the code, we take this phenomenon into account as two first order transformations, (E-45) and (E-46) for oxygen, (E-47) and (E-48) for hydrogen. The different species are identified as H_2 and O_2 when dissolved in water and as H_{2g} and O_{2g} in the gas phase. Kinetic constants of forward transformations (from dissolved form to gas phase) are arbitrary set to 10^6 s^{-1}, to ensure that mass transfer would not be the rate-determining step. Kinetic constants of backward transformations (from gas phase to dissolved species) are calculated from Henry's law constants at the considered temperature.

IV.B. Simulation results

Figure 2 displays the experimental evolution of the concentration of hydrogen and oxygen in the gas phase as well as the simulated results. Although the general trend of the evolution of the simulated results is comparable with experimental data, the simulated concentrations in both gaseous species are higher than the experimental ones. Moreover, difference between both values increases with time. We have checked that uncertainties on kinetic constants and radiolytic primary yields are not enough to explain this difference.

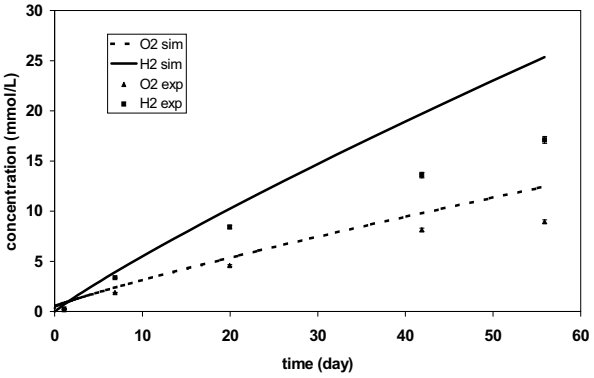

Fig. 2. Experimental and simulated evolution of the concentration of hydrogen and oxygen in the experiment with 300 mL of water.

IV.C. Simulation of recombination in gas phase

In order to fit experimental data, we have to take into account an additional mechanism involving reactions in gas phase that reflect recombination of hydrogen and oxygen to form water. This mechanism should be similar to those involving hydrogen combustion or in catalytic hydrogen – oxygen combination. Reactions (E-49) to (E-57) represent formation of water from gas phase species[7]. The rate-determining step is supposed to be hydrogen molecules dissociation in hydrogen radicals in gas phase (E-49). In the present case, this homolytic dissociation should be initiated by β particles from tritium decay in the gas phase. As we have experimentally proved that the concentration of tritiated hydrogen, HT, is negligible (see table I), the unique source of radiation in the gas phase is tritiated water vapour that is in equilibrium with the liquid phase (about 10^{-3} mmol·L^{-1} of HTO molecules in the gaseous phase). Kinetic rates of reactions (E-50) to (E-57) are taken from literature. Concerning homolytic dissociation of molecular hydrogen, the production of hydrogen radicals should be rigorously quantified as a radiochemical phenomenon, that is considering a radiolytic yield and a dose. Nevertheless, as the code is originally conceived for single-phase systems, it is impossible to simulate radiochemical phenomenon in both phases. Thus, we associated to this reaction a pseudo kinetic constant that reflects dose rate in gas phase to take into account radiochemical production of hydrogen atoms.

Table II. Reactions and kinetics constants (in s^{-1} for first order reactions, in $L.mol^{-1}.s^{-1}$ for second order reactions) in used for simulation[8-9].

N°	Reaction	k	N°	Reaction	k
E-1	$H_2O \rightarrow H^+ + OH^-$	$2.57 \cdot 10^{-5}$	E-30	$OH^\bullet + H_2 \rightarrow H^\bullet + H_2O$	$4.0 \cdot 10^{7}$
E-2	$H^+ + OH^- \rightarrow H_2O$	$1.43 \cdot 10^{11}$	E-31	$OH^\bullet + H_2O_2 \rightarrow H_2O + HO_2^\bullet$	$7.0 \cdot 10^{8}$
E-3	$H^\bullet + OH^- \rightarrow e_{aq}^-$	$2.2 \cdot 10^{7}$	E-32	$OH^\bullet + HO_2^- \rightarrow H_2O + O_2^-$	$7.0 \cdot 10^{9}$
E-4	$H^+ + e_{aq}^- \rightarrow H_2O + H^\bullet$	$2.5 \cdot 10^{10}$	E-33	$OH^\bullet + HO_2^\bullet \rightarrow O_2 + H_2O$	$7.0 \cdot 10^{9}$
E-5	$OH^\bullet + OH^- \rightarrow O^- + H_2O$	$1.2 \cdot 10^{10}$	E-34	$OH^\bullet + O_2^- \rightarrow O_2 + OH^-$	$1.0 \cdot 10^{10}$
E-6	$O^- + H_2O \rightarrow OH^\bullet + OH^-$	$1.66 \cdot 10^{6}$	E-35	$OH^\bullet + O_3^- \rightarrow HO_2^\bullet + O_2^-$	$8.5 \cdot 10^{9}$
E-7	$H_2O_2 + OH^- \rightarrow HO_2^- + H_2O$	$5.0 \cdot 10^{8}$	E-36	$O^- + H_2 \rightarrow e_{aq}^-$	$1.0 \cdot 10^{10}$
E-8	$HO_2^- + H^+ \rightarrow H_2O_2$	$3.4 \cdot 10^{4}$	E-37	$O^- + H_2O_2 \rightarrow O_2^- + H_2O$	$5.0 \cdot 10^{8}$
E-9	$HO_2^\bullet \rightarrow H^+ + O_2^-$	$8 \cdot 10^{5}$	E-38	$O^- + HO_2^- \rightarrow OH^- + O_2^-$	$3.0 \cdot 10^{7}$
E-10	$H^+ + O_2^- \rightarrow HO_2^\bullet$	$5 \cdot 10^{10}$	E-39	$O^- + O_2 \rightarrow O_3^-$	$3.8 \cdot 10^{9}$
E-11	$H^\bullet + H_2O \rightarrow H_2 + OH^\bullet$	$5.5 \cdot 10^{2}$	E-40	$O^- + O_3^- \rightarrow 2O_2^-$	$7.0 \cdot 10^{8}$
E-12	$H^\bullet + H^\bullet \rightarrow H_2$	$5.0 \cdot 10^{9}$	E-41	$O_3^- \rightarrow O^- + O_2$	$3.3 \cdot 10^{3}$
E-13	$H^\bullet + e_{aq}^- \rightarrow H_2 + OH^-$	$2.5 \cdot 10^{10}$	E-42	$HO_2^\bullet + O_2^- \rightarrow O_2 + HO_2^-$	$9.7 \cdot 10^{7}$
E-14	$H^\bullet + OH^\bullet \rightarrow H_2O$	$7 \cdot 10^{9}$	E-43	$HO_2^\bullet + HO_2^\bullet \rightarrow O_2 + H_2O_2$	$8.3 \cdot 10^{5}$
E-15	$H^\bullet + H_2O_2 \rightarrow H_2O + OH^\bullet$	$1.5 \cdot 10^{10}$	E-44	$O_3^- + H^+ \rightarrow O_2 + OH^\bullet$	$9.0 \cdot 10^{10}$
E-16	$H^\bullet + HO_2^\bullet \rightarrow H_2O_2$	$2.0 \cdot 10^{10}$	E-45	$O_2 \rightarrow O_{2g}$	$1.0 \cdot 10^{6}$
E-17	$H^\bullet + HO_2^- \rightarrow OH^\bullet + OH^-$	$1.38 \cdot 10^{9}$	E-46	$O_{2g} \rightarrow O_2$	$6.2 \cdot 10^{5}$
E-18	$H^\bullet + O_2 \rightarrow HO_2^\bullet$	$1.4 \cdot 10^{10}$	E-47	$H_2 \rightarrow H_{2g}$	$1.0 \cdot 10^{6}$
E-19	$H^\bullet + O_2^- \rightarrow HO_2^-$	$2.0 \cdot 10^{10}$	E-48	$H_{2g} \rightarrow H_2$	$3.8 \cdot 10^{5}$
E-20	$H^\bullet + O^- \rightarrow OH^-$	$2.0 \cdot 10^{10}$	E-49	$H_{2g} \rightarrow H_g^\bullet + H_g^\bullet$	$2.0 \cdot 10^{-7}$
E-21	$e_{aq}^- + e_{aq}^- \rightarrow H_2 + 2OH^-$	$5.5 \cdot 10^{9}$	E-50	$H_g^\bullet + H_g^\bullet \rightarrow H_{2g}$	$4.0 \cdot 10^{7}$
E-22	$e_{aq}^- + OH^\bullet \rightarrow OH^- + H_2O$	$3.0 \cdot 10^{10}$	E-51	$H_g + O_{2g} \rightarrow HO_{2g}^\bullet$	$4.5 \cdot 10^{8}$
E-23	$e_{aq}^- + H_2O_2 \rightarrow OH^\bullet + OH^- + H_2O$	$1.3 \cdot 10^{10}$	E-52	$H_g^\bullet + HO_{2g}^\bullet \rightarrow 2OH_g^\bullet$	$6.5 \cdot 10^{10}$
E-24	$e_{aq}^- + O_2 \rightarrow O_2^- + H_2O$	$1.9 \cdot 10^{10}$	E-53	$HO_{2g}^\bullet + HO_{2g}^\bullet \rightarrow H_2O_2 + O_{2g}$	$2.0 \cdot 10^{9}$
E-25	$e_{aq}^- + O^- \rightarrow 2OH^-$	$1.5 \cdot 10^{10}$	E-54	$OH_g^\bullet + OH_g^\bullet \rightarrow H_2O_2$	$4.0 \cdot 10^{9}$
E-26	$e_{aq}^- + O_2^- \rightarrow HO_2^- + OH^-$	$1.2 \cdot 10^{10}$	E-55	$H_g^\bullet + OH_g^\bullet \rightarrow H_2O$	$1.0 \cdot 10^{10}$
E-27	$e_{aq}^- + HO_2^- \rightarrow O^- + OH^- + H_2O$	$3.5 \cdot 10^{9}$	E-56	$OH_g^\bullet + HO_{2g}^\bullet \rightarrow H_2O + O_{2g}$	$6.0 \cdot 10^{10}$
E-28	$OH^\bullet + OH^\bullet \rightarrow H_2O_2$	$5.5 \cdot 10^{9}$	E-57	$OH_g^\bullet + H_{2g} \rightarrow H_2O + H_g^\bullet$	$4.0 \cdot 10^{3}$
E-29	$OH^\bullet + O^- \rightarrow HO_2^-$	$2.0 \cdot 10^{9}$			

Table III. Values of the primary radiolytic yields used for simulation.

Species	Radiolytic yield (species/100 eV)
H_2	0.53
e^-_{aq}	2.42
H	0.48
OH^-	0.00
H_2O	-6.38
H^+	2.42
OH	2.00
H_2O_2	0.98
HO_2	0.00

Figure 3 displays both the experimental results and simulation that takes into account gas phase recombination. Whatever the volume of water, the pseudo kinetic constant for molecular hydrogen formation that allows fitting experimental results is $2 \cdot 10^{-7}$ s^{-1}. This value is suitable only with the considered volumic activity of tritiated water. The study of the relation between water volumic activity and the value of the pseudo kinetic constant, that could allow to identify the initial mechanism of the interaction between β radiation and gaseous molecular hydrogen, is not in the scope of the present work.

V. INTERPRETATION OF RADIOLYSIS MECHANISM

In order to understand the mechanism of self-radiolysis of tritiated water, the chemical system used to simulate this phenomenon has been simplified by suppressing the reactions that have a negligible contribution to radiolytic gas formation. Figure 4 shows a simulation realised with both complete and simplified systems. This simplified systems contains the acido basic equilibrium, (19) to (28), reactions representing mass transfer between the two phases, (63) to (66), reactions representing recombination in gas phase, (67) to (75), and only the eight following reactions involving:

- consumption of hydrogen:

$$OH^\bullet + H_2 \rightarrow H^\bullet + H_2O \qquad k = 4.0 \cdot 10^7 \quad (11)$$

- consumption of hydrogen peroxide (acid or basic form):

$$H^\bullet + H_2O_2 \rightarrow H_2O + OH^\bullet \qquad k = 1.5 \cdot 10^{10} \quad (12)$$

$$e^-_{aq} + H_2O_2 \rightarrow OH^\bullet + OH^- + H_2O \qquad k = 1.3 \cdot 10^{10} \quad (13)$$

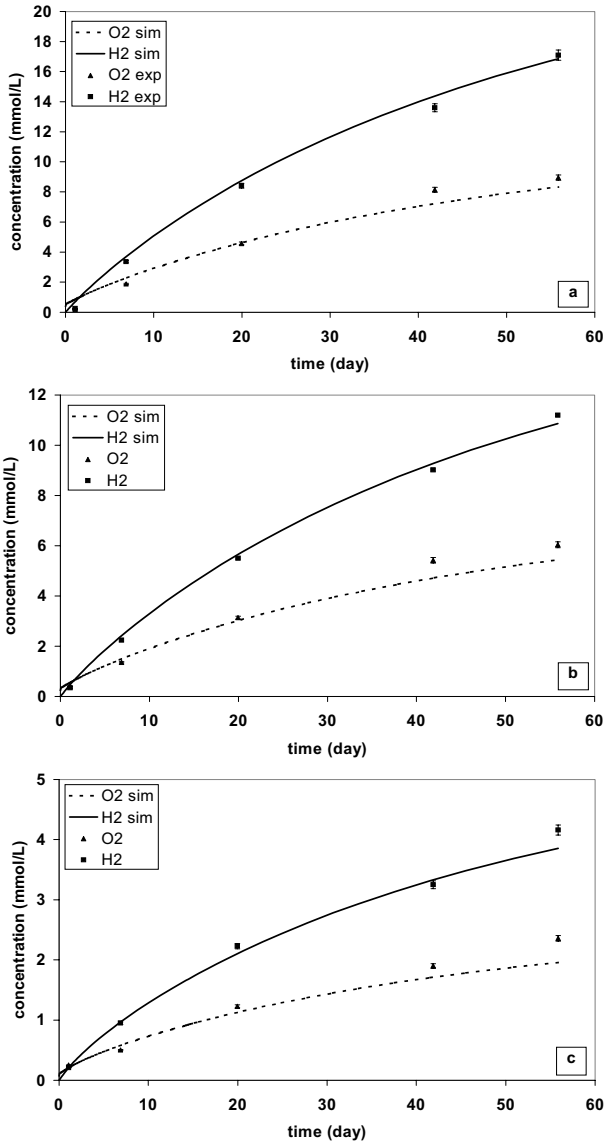

Fig. 3. Experimental and simulated evolution of the concentration of hydrogen and oxygen when taking into account gas phase recombination, with different volumes of water. (a) 300 mL. (b) 250 mL. (c) 125 mL.

$$OH^\bullet + H_2O_2 \rightarrow H_2O + HO_2^\bullet \qquad k = 7.0 \cdot 10^8 \quad (14)$$

$$OH^\bullet + HO_2^- \rightarrow H_2O + O_2^- \qquad k = 7.0 \cdot 10^9 \quad (15)$$

- formation of oxygen:

$$HO_2^\bullet + O_2^- \rightarrow O_2 + HO_2^- \qquad k = 9.7 \cdot 10^7 \quad (16)$$

- consumption of oxygen:

$$H^{\bullet} + O_2 \rightarrow HO_2^{\bullet} \qquad k = 1.4 \cdot 10^{10} \quad (17)$$

$$e_{aq}^{-} + O_2 \rightarrow O_2^{-} + H_2O \qquad k = 1.9 \cdot 10^{10} \quad (18)$$

From these results, we can conclude that molecular hydrogen is only produced during primary radiolysis steps and reacts only with hydroxide radicals. Hydrogen peroxide, that is also a primary product of radiolysis, reacts with hydroxide radicals to form hydroperoxide radicals. These radicals are precursors of molecular oxygen that is not a primary product of radiolysis. Moreover, oxygen reacts with hydrogen radicals and aqueous electrons.

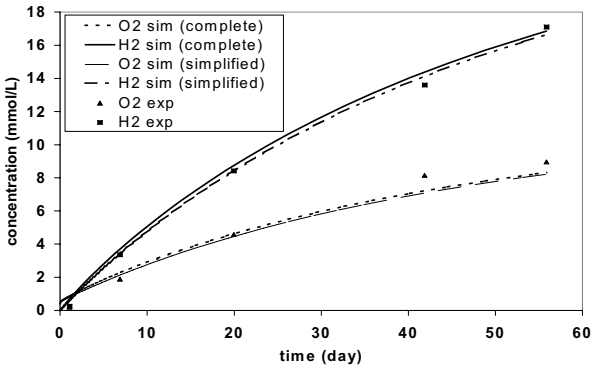

Fig. 4. Comparison of simulation of the evolution of the concentration of hydrogen and oxygen with complete and simplified chemical systems.

VI. CONCLUSION AND OUTLOOK

The results of this work show that simulation of self-radiolysis of weak volumic activity chemically pure tritiated water requires to take into account not only the radiochemical and the chemical processes that take place in the liquid phase, but also recombination of hydrogen and oxygen in the gas phase. This phenomenon, that is supposed to be initiated by β radiation produced by tritiated water vapour, should be investigated more extensively in a further step to identify its basic mechanisms and to allow a more precise prediction of pressure increase in storage vessels.

Simulation has also allowed to identify the main reactions that take place in tritiated water self-radiolysis in the case of chemically pure water. Moreover, tritiated water produced by detritiation plants is often polluted by ionic species such as chloride, iron, chromium, and nickel. In the continuity of this work, the study of the influence of the species should be considered. Finally, tritiated water is commonly stored onto zeolite. Thus, the study should also be extended to this form.

ACKNOWLEDGMENTS

The authors would like to thank the Burgundy Regional Council for its financial support to this project.

REFERENCES

[1] A. O. ALLEN, *The Radiation Chemistry of Water and Aqueous Solutions*, D. Van Nostrand Compagny, New York (1961).

[2] I. G. DRAGANIC and Z.D. DRAGANIC, *The Radiation Chemistry of Water*, Academic Press, New York (1971).

[3] J. K. T. SPINKS and R. J. WOODS, *An Introduction to Radiation Chemistry*, Wiley Interscience, New York (1990).

[4] E. COLLINSON, F. S. DAINTON and J. KROH, "The Radiation Chemistry of Aqueous Solutions II. Radical and Molecular Yields for Tritium Beta-particule", *Proceedings of the Royal Society*, **265A**, 422 (1962).

[5] T. STOLZ, PhD thesis, *Etude expérimentale de l'auto-radiolyse de l'eau tritiée. Approche expérimentale et simulation*, Université de Bourgogne, Dijon, 2003.

[6] R. VIALLARD, Nouveau Traité de Chimie Minérale

[7] P. KIRKEGAARD and E. BJERGBAKKE, *Chemsimul: a Simulation for Chemical Kinetics*, RISO-R-1085, Roskilde (2001).

[8] E. BJERGBAKKE, K. SEHESTED, O. LANG RASMUSSEN and H. CHRISTENSEN, *Input Files for Computer Simulation of Water Radiolysis*, RISO-M-2430, Roskilde (1984).

[9] A. B. ROSS, W. G. MALLARD, W. P. HELMAN, G. V. BUXTON, R. E. HUIE and P. NETA, *NDRL-NIST Solution Kinetic Database version 2.0*, NIST, Gauthersburg (1994).